On the role of the ν_τ appearance in DUNE in constraining standard neutrino physics and beyond

A. Ghoshal,[a,b] A. Giarnetti[a] and D. Meloni[a]

[a]*Dipartimento di Matematica e Fisica, Università di Roma Tre,*
Via della Vasca Navale 84, 00146 Rome, Italy

[b]*INFN, Laboratori Nazionali di Frascati,*
C.P. 13, 00044 Frascati, Italy

E-mail: anishghoshal1@gmail.com, giarnetti.alessio@gmail.com,
davide.meloni@uniroma3.it

ABSTRACT: We consider the $\nu_\mu \to \nu_\tau$ appearance channel in the future Deep Underground Neutrino Experiment (DUNE) which offers a good statistics of the ν_τ sample. In order to measure its impact on constraining the oscillation parameters, we consider several assumptions on the efficiency for ν_τ charged-current signal events (with subsequent $\tau \to e$ decay) and the related backgrounds and study the effects of various systematic uncertainties. Two different neutrino fluxes have been considered, namely a CP-violation optimized flux and a ν_τ optimized flux.

Our results show that the addition of the $\nu_\mu \to \nu_\tau$ appearance channel does not reduce the current uncertainties on the standard 3-ν oscillation parameters while it can improve in a significant way the sensitivity to the Non-Standard Interaction parameter $|\epsilon_{\mu\tau}|$ and to the new mixing angle θ_{34} of a sterile neutrino model of the $3 + 1$ type.

Contents

1 Introduction

Neutrino experiments over the last 20 years have established the phenomenon of neutrino oscillations and now we are in the era of precision measurements in the leptonic sector. Although experiments detecting neutrinos from many sources were able to constrain with a very good precision the oscillation parameters, there are still some open questions. In particular, future experiments will be focused on measuring the CP violation in the lepton sector and on determining the sign of the atmospheric mass splitting. Another ambiguity is present in the value of the mixing angle θ_{23}, since we still do not know in which octant this angle lies.

Beside checking for the Standard Physics, neutrinos can also be used to test Beyond Standard Model (BSM) physics. Among several scenarios, Non-Standard neutrino Interactions (NSI) with matter [1, 2] and the existence of a fourth sterile neutrino have recently attracted a lot of interest, especially in connection to the ability of long baseline neutrino experiments (LBL) to probe for them [3]–[25].

One of the most powerful neutrino experiment that will be built in the near future is the DEEP Underground Neutrino Experiment (DUNE) [26, 27]. This experiment consists of a baseline of 1300 km, planned across two sites in North America; the near site, situated at

the Fermi National Accelerator Laboratory (FNAL), Batavia in Illinois, will hosts the Long Baseline Neutrino Facility (LBNF) and the Near Detector (ND). LBNF [28] will provide a GeV-scale ν_μ beam (with contamination of ν_e) at 1.2 MW, later upgradeable to 2.4 MW. At the opposing end of the baseline, the far site in Sanford Underground Research Facility (SURF) in South Dakota will house four 10 kt Liquid Argon Time Projection Chambers (LArTPC) as the Far Detector (FD).

The DUNE neutrino beam will be able to operate in the Forward Horn Current (FHC, ν mode) and Reverse Horn Current (RHC, $\bar{\nu}$ mode) modes, in order to look for oscillations of both neutrinos and anti-neutrinos.

DUNE has been designed in order to answer all the questions mentioned before. The proposed neutrino flux (to which we will refer throughout the rest of the paper as the *the standard flux* [29]) will be optimized for the CP violation measurement and for this reason will provide a relatively large sample of ν_e coming from $\nu_\mu \to \nu_e$ oscillations. However this experiment will also be able to collect a huge ν_τ sample, even if most of the neutrinos will not reach the threshold energy of 3.4 GeV for the τ production.

Motivated by the interest on τ neutrinos recently triggered by the observation of 8 ν_τ interactions by the OPERA experiment[1] [30–32], in this paper we consider in detail the effect of adding the $\nu_\mu \to \nu_\tau$ appearance channel to the more widely used ν_e appearance and ν_μ disappearance modes[2] in the study of the sensitivity of the DUNE experiment to the oscillation parameters of the standard 3-ν framework as well as in the investigation of the parameter space of the NSI and of the sterile $3 + 1$ neutrino models. Differently from [34], which focused on the τ hadronic decays, we consider the $\tau \to e$ leptonic decay. In our numerical simulations, performed with the help of the GLoBES software [35, 36], we take into account various detection efficiencies, signal to background ratios (S/B) and systematic uncertainties and explore the performances of the DUNE far detector not only for the standard flux but also for a ν_τ-*optimized flux* as described in [37] and [38]. In both cases we have considered 3.5 years of data taking in the neutrino mode and 3.5 years in the anti-neutrino modes for a total of 7 years.

The paper is organized as follows: in section 2 we describe the neutrino fluxes and the efficiencies, systematics and backgrounds of the ν_τ appearance channel; in section 3 we focus on the sensitivity reaches of the DUNE detector on the standard oscillation parameters allowed by the ν_τ channel alone and for both standard and optimized fluxes. section 4 is devoted to investigate the impact of this additional channel on NSI parameter sensitivities while in section 5 we study in detail the sterile neutrino case. We draw our conclusion in section 6.

2   On the simulation of the ν_τ appearance in DUNE

In this section we specify the differences between the two fluxes used in our numerical simulations and comment on the values for efficiencies, systematics and backgrounds of the ν_τ appearance channel taken into account while evaluating the DUNE performance on the mixing parameters measurements, computed for $3.5 + 3.5$ years of running time.

---

[1]OPERA observed 10 ν_τ candidates, with an expected background of 2 events.

[2]An introductory study about the ν_τ appearance in DUNE can be found in [33].

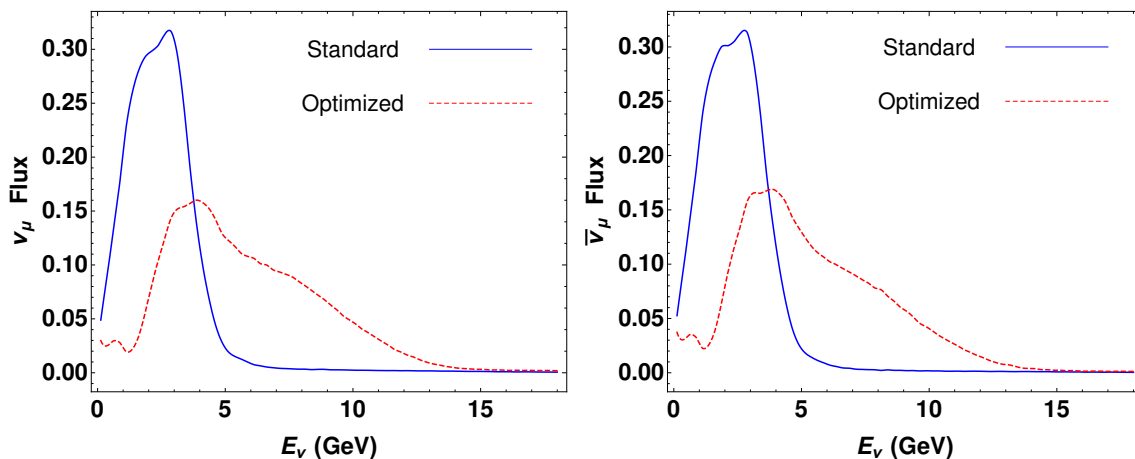**Figure 1**. ν_μ (left panel) and $\bar{\nu}_\mu$ (right panel) fluxes in arbitrary units. Standard (blue, solid) and optimized (red, dashed) cases are shown.

	Standard Flux		Optimized Flux	
	FHC mode	RHC mode	FHC mode	RHC mode
ν_μ CC	30175	3225	85523	4933
$\bar{\nu}_\mu$ CC	1025	9879	1256	26221
ν_e CC	371	136	856	258
$\bar{\nu}_e$ CC	44	109	84	215

Table 1. Expected ν_e and ν_μ un-oscillated CC event rates at the DUNE 40-kt far detector for a run-time of total 7 years (3.5 years in neutrino mode and 3.5 years in anti-neutrino mode). Numbers refer to the two flux options analyzed in this paper.

2.1 Fluxes

The two ν_μ fluxes discussed in this paper have been displayed in figure 1; in both panels (neutrinos on the left, anti-neutrino on the right panel), the blue-solid line refers to the DUNE standard flux [29], which is said to be optimized to maximize sensitivity for CP violation measurements [27], while the red-dashed case refers to the optimized ν_τ scenario of [37] and [38].

The standard flux consists of LBNF beam delivering 1.47×10^{21} protons on target (POT) per year with 80 GeV energy running with 1.07 MW beam power and having 1.5 m NuMI (Neutrinos at the Main Injector) style target. The τ optimized flux is as per proposed by the DUNE collaboration [37] and it consists of 1.1×10^{21} protons on target (POT) per year with 120 GeV energy running with 1.2 MW beam power and having 1 m NuMI style target. The expected un-oscillated charged current (CC) event rates are reported in table 1; for any of the flux options, we computed the ν_e and ν_μ events (together with their CP conjugate modes) when the LBNF beam is working in the FHC and RHC modes. Notice that for the normalization of the tau optimized flux we referred to the number of ν_τ events as reported in ref. [38].

We observe that the optimized flux in each of the ν and $\bar{\nu}$ modes gives a larger number of events. This is mainly due to the more energetic protons involved than in the standard flux which produce higher energy neutrinos and thus implies larger neutrino-nucleus cross sections.

2.2 Efficiencies, systematics and backgrounds

In this section we quote the relevant efficiencies, systematics and backgrounds of the transition channels included in our numerical simulations.

For the standard flux and the ν_e appearance and ν_μ disappearance channels, we strictly follow ref. [27]: the appearance modes in the proposed DUNE experiment have independent systematic uncertainties of 2% each, while the ν_μ and $\bar{\nu}_\mu$ disappearance modes have independent systematic uncertainties of 5%. The systematic uncertainties for the backgrounds are 5% for ν_e and ν_μ CC events, 10% for NC events and 20% for ν_τ events. For the standard flux all DUNE collaboration post smearing matrices generated using the DUNE Fast Monte Carlo (MC) [27] have been used for the ν_e appearance and ν_μ disappearance channels to set the detection efficiencies.

For the optimized flux studies, since to our knowledge there are no official DUNE MC simulations available, background and signal efficiencies for ν_e appearance and ν_μ disappearance have been set to constant values, obtained from averaging the efficiency factors in various energy bins quoted in [27]. For both fluxes, the energy resolution of the detector is described by resolution functions given by the collaboration in ref. [27].

As for the ν_τ appearance detection, for a *zeroth order* study we envisage the DUNE detector to be similar to the ICARUS one. The ν_τ appearance sample is composed of ν_τ CC interactions resulting from $\nu_\mu \rightarrow \nu_\tau$ oscillations. Backgrounds to this channel come from the ν_e CC, ν_μ CC and NC interactions. Focusing on the leptonic decay of the tau generated by ν_τ CC interactions, we consider the electron channel only (18% branching fraction [39]) since muonic tau decays are affected by large ν_μ CC background. From the ICARUS proposal [40] it is clear that choosing the right kinematic cuts, the electron channel background can be reduced to only ν_e CC events coming from two main components, which are the intrinsic ν_e beam and $\nu_\mu \rightarrow \nu_e$ oscillation.[3] Due to the spatial resolution of the DUNE LArTPC detector, very short tau tracks will not be recognized, and for this reason ν_e CC background cannot be avoided. In this paper, for both standard and optimized neutrino fluxes, the overall ν_τ and $\bar{\nu}_\tau$ appearance signal efficiency has been set to two distinct values (including the branching fraction), that are 6% [41] and, in order to show the full potential of the electron channel, also the maximum reachable efficiency of 18%. The former case has to be considered as a pessimistic case, being related to the expected selection efficiency of an old-generation detector like ICARUS; in fact, we expect DUNE to have better performances in reconstructing electrons tracks and in distinguishing electrons coming from tau decays. On the other hand, the latter efficiency of 18% has to be considered as an optimistic assumption, since it corresponds to DUNE able to reconstruct and recognize all produced electrons.

---

[3]There is negligible intrinsic ν_τ component in the beam.

The number of the ν_e CC background has been set to a constant value as to avoid the parameter dependence of the rates that, with such a comparatively small number of ν_τ events, can overshadow the effect of the signal in the simulations; in particular, such a background has been chosen in order to reproduce, at the best fit parameter values, two S/B ratios discussed for ICARUS: 18.6 [40] and 2.45 [41]. In order to show the impact of ν_τ systematic uncertainties on the results, we study the situation where such an uncertainty for ν_τ signal events is fixed to the same value used by the DUNE collaboration when ν_τ CC are considered as a background to the ν_e appearance and ν_μ disappearance channels, that is 20%, and also the situation where an optimistic 10% is taken into account.

Expected total rates for ν_τ, $\bar{\nu}_\tau$ and ν_e, $\bar{\nu}_e$ CC events for both fluxes are shown in tables 3 and 4.

3 The case of Standard Physics

The $\nu_\mu \to \nu_\tau$ oscillation probability, among others, was calculated in [42]. Neglecting terms containing the solar mass difference $\Delta m_{21}^2 = m_2^2 - m_1^2$ and the small $\sin\theta_{13}$, in vacuum such a probability reads:

$$P_{\mu\tau} \approx \cos^4\theta_{13}\sin^2 2\theta_{23}\sin^2\left(\frac{\Delta m_{31}^2 L}{4E}\right) . \tag{3.1}$$

Eq. (3.1) shows that the ν_τ appearance channel is particularly sensitive to θ_{23} and to the atmospheric mass-squared splitting $\Delta m_{31}^2 = m_3^2 - m_1^2$. However, also the other two channels are expected to be sensitive to the same two parameters since, neglecting solar terms, we have:

$$P_{\mu e} \approx 4\sin^2\theta_{13}\cos^2\theta_{13}\sin^2\theta_{23}\sin^2\left(\frac{\Delta m_{31}^2 L}{4E}\right) , \tag{3.2}$$

and

$$P_{\mu\mu} \approx 1 - (\sin^2 2\theta_{23}\cos^4\theta_{13} + \sin^2 2\theta_{13}\sin^2 2\theta_{23})\sin^2\left(\frac{\Delta m_{31}^2 L}{4E}\right) . \tag{3.3}$$

In DUNE the mean neutrino energy in the standard flux has been chosen in order to maximize the atmospheric term; since the minimum ν_τ energy needed to be converted in a τ lepton is around $3.4\,\mathrm{GeV}$, the number of ν_e and ν_μ events will be much bigger than the number of ν_τ CC. For this reason, we expect that constraints on θ_{23} and Δm_{31}^2 will be mainly set by $\nu_\mu \to \nu_e$ and $\nu_\mu \to \nu_\mu$ channels. Notice also that next terms in the Δm_{21}^2 and θ_{13} of eq. (3.1) would exhibit a $\sin\delta_{CP}$ dependence, so we expect this channel to be also partially sensitive to CP violation searches. However, due to the very large leading term, the changes in probability due to the CP violation phase will be comparatively very small and definitely less important than the corresponding CP violating terms in $P_{\mu e}$.

In summary, considering the $\nu_\mu \to \nu_\tau$ oscillation probability and the lack of statistics, the ν_τ appearance channel is expected to have a negligible impact on standard physics studies.

Parameter	Central Value	Relative Uncertainty
θ_{12}	0.59	2.3%
θ_{23} (NH)	0.866	2.0%
θ_{13}	0.15	1.4%
Δm^2_{21}	$7.39 \times 10^{-5}\,\mathrm{eV}^2$	2.8%
Δm^2_{31} (NH)	$2.525 \times 10^{-3}\,\mathrm{eV}^2$	1.3%

Table 2. Central values and relative uncertainty of neutrino oscillation parameters from a global fit to neutrino oscillation data [43]. As in [26], for non-Gaussian parameter θ_{23} the relative uncertainty is computed using 1/6 of the 3σ allowed range. Normal mass hierarchy (NH) is assumed. Throughout the analysis presented in this paper, we assumed true values of δ_{CP} to be 215° as per ref. [43]. We have used these values as central values for our simulation unless otherwise stated explicitly in the text.

ν **mode**	
ν_τ Signal	277
$\bar{\nu}_\tau$ Signal	26
Total Signal	303
$\nu_e + \bar{\nu}_e$ CC Bkg (beam)	333 + 38
$\nu_e + \bar{\nu}_e$ CC Bkg (oscillation)	1753 + 12

$\bar{\nu}$ **mode**	
ν_τ Signal	68
$\bar{\nu}_\tau$ Signal	85
Total Signal	153
$\nu_e + \bar{\nu}_e$ CC Bkg (beam)	117 + 104
$\nu_e + \bar{\nu}_e$ CC Bkg (oscillation)	90 + 188

Table 3. Expected total number of events after oscillation at the 40-kt far detector for Signals and Backgrounds (Bkg) obtained using no selection efficiencies hypothesis in the case of the standard flux and for Normal Hierarchy (NH). $\delta_{CP} = 215°$ is assumed [43]. The events correspond to DUNE running for a total of 7 years (3.5 years in neutrino mode and 3.5 years in anti-neutrino mode).

3.1 Expected rates for signal and backgrounds

In this section we estimate the event rates for the ν_τ appearance in DUNE. We have used mixing parameters with their error bars from [43] which we summarize in table 2. The expected rates of the ν_τ signal and background (Bkg) from the two fluxes considered here are reported in table 3 for the standard flux and in table 4 for the optimized flux. These tables show the total number of expected ν_τ and ν_e CC events in DUNE without considering any detection strategy. Using the efficiencies and S/B values discussed in the previous section, the number of signal and background events in every configuration considered in this paper can be obtained. In both tables we specify the two sources of electron backgrounds coming from the intrinsic ν_e component of the beam, $[\nu_e \oplus \bar{\nu}_e$ CC Background (beam)], and from $\nu_\mu \to \nu_e$ oscillations, [CC Background (oscillation)].

These numbers must be compared with a total of 2043 (2369) $\nu_\mu \to \nu_e \oplus \bar{\nu}_\mu \to \bar{\nu}_e$ CC signal events for the standard (optimized) flux and with a total of 14206 (67143) $\nu_\mu \to \nu_\mu \oplus \bar{\nu}_\mu \to \bar{\nu}_\mu$ CC signal events.

We clearly observe that the DUNE experiment is able by itself to provide a τ sample around 300 events in FHC mode and 150 in RHC mode because of the generous ν_μ flux components above the tau production threshold. On top of that, as per the plan for the op-

ν mode			$\bar{\nu}$ mode	
ν_τ Signal	2673		ν_τ Signal	98
$\bar{\nu}_\tau$ Signal	34		$\bar{\nu}_\tau$ Signal	983
Total Signal	2707		Total Signal	1081
$\nu_e + \bar{\nu}_e$ CC Bkg (beam)	688 + 63		$\nu_e + \bar{\nu}_e$ CC Bkg (beam)	176 + 177
$\nu_e + \bar{\nu}_e$ CC Bkg (oscillation)	1958 + 11		ν_e CC Bkg (oscillation)	76 + 324

Table 4. Same as table 4 but for the optimized flux.

timized flux, there is a huge gain in statistics by roughly a factor of 10 with respect to standard taus, thereby justifying the possibility to explore scenarios of new physics with taus.

3.2 Details on the χ^2 definition

The confidence regions involving the sensitivity of the measurement of the oscillation parameters are determined based on the standard pull method [44–46] as implemented in GLoBES. The χ^2 is calculated by the minimizing over the nuisance parameters $\vec{\xi}$. For every transition channel c with energy bin i (in the case of DUNE the number of energy bins suggested by the collaboration is 71 [29]), a Poissonian χ^2 distribution is used of the form:

$$\chi_c^2 = \sum_i 2\left(f_{c,i}(\vec{\theta},\vec{\xi}) - O_{c,i} + O_{c,i} \ln \frac{O_{c,i}}{f_{c,i}(\vec{\theta},\vec{\xi})} \right). \tag{3.4}$$

For the i-th energy bin for a given channel c, and for a set of oscillation parameters $\vec{\theta}$ and nuisance parameters $\vec{\xi}$, $f_{c,i}(\vec{\theta},\vec{\xi})$ is the predicted number of events and $O_{c,i}$, is the observed event rate i.e., the event rate considering assumed true values of the oscillation parameters. Both $f_{c,i}$ and $O_{c,i}$ receive contributions from different sources s, that usually involve signal and background rates given by $R_{c,s,i}(\vec{\theta})$, such that

$$f_{c,i}(\vec{\theta},\vec{\xi}) = \sum_s \left(1 + a_{c,s}(\vec{\xi}) \right) R_{c,s,i}(\vec{\theta}). \tag{3.5}$$

The auxiliary parameters $a_{c,s}$ have the form $a_{c,s} \equiv \sum_k w_{c,s,k}\, \xi_k$, in which the coefficients $w_{c,s,k}$ assume the values 1 or 0 corresponding respectively to a particular nuisance parameter ξ_k affecting or not affecting the contribution from the source s to channel c.

Therefore, the χ^2 is given by in total by:

$$\chi^2 = \min_\xi \left\{ \sum_c \chi_c^2 + \left(\frac{\xi_N}{\sigma_N} \right)^2 \right\},$$

where the overall signal normalization is represented respectively by the last term known as the pull term. The different values used for σ_N have been quoted in section 2.2 (for both signal and background).

3.3 Numerical results

Standard flux. In this section we exclusively use the standard flux configurations with an exposure of $3.5 + 3.5$ years for investigating the sensitivity and correlation among the standard physics parameters obtained from the ν_τ appearance channel.

In figure 2 we report correlation plots in the planes $(\theta_{13}, \Delta m_{31}^2)$ (top left), $(\theta_{23}, \Delta m_{31}^2)$ (top right) and $(\theta_{13}, \theta_{23})$ (bottom left), while the $\Delta\chi^2 = \chi^2 - \chi_{\min}^2$ versus Δm_{31}^2 is shown in the bottom right panel. In each panel we show four different cases: (Red, DotDashed) refers to ν_τ detection efficiency of 6% and $S/B = 2.45$, (Brown, Dashed) to the same S/B but 18% of detection efficiencies while the (Blue, Dotted) and the (Black, Solid) lines refer to 6% and 18%, respectively, and the same $S/B = 18.6$. Contours are at 68% confidence level (CL) and are obtained assuming a 10% systematic error on the signal.

It is clear that when the ν_τ detection efficiency is increased from 6% to 18%, the number of signal events is increased and this results in smaller allowed regions in the correlation plots. The allowed range for θ_{13} can be reduced by up to 18%, as we can see in the correlation plot in the $(\theta_{13}, \Delta m_{31}^2)$ plane. On the other hand, the θ_{23} range can be reduced approximately by 15%, as shown in the $(\theta_{23}, \Delta m_{31}^2)$ plane. For Δm_{31}^2, instead, an improvement of approximately 30% can be reached passing from the worst case ($S/B = 2.45$, with ν_τ detection efficiency at 6%) to the best one ($S/B = 18.6$, with ν_τ detection efficiency at 18%). Notice that the OPERA experiment measured $\Delta m_{31}^2 = (2.7 \pm 0.7) \times 10^{-3}\,\mathrm{eV}^2$ [32, 48] while the DUNE setup here discussed with an 18% τ detection efficiency reaches a much better relative uncertainty of about 8%.

Also a larger S/B gives a better sensitivity to the mixing parameters: in particular, for $S/B = 18.6$ the correlation plots show a reduction of the mixing angles allowed ranges of approximately 5% if compared to the case $S/B = 2.45$. Roughly the same reduction can be noticed in the relative uncertainty of Δm_{31}^2. Thus we conclude that an increase in efficiency allows a better performance of the DUNE detector than a larger S/B.

In figure 3 we depict the same plots as in figure 2 but with 20% systematic uncertainty on the signal. We see that doubling the systematic uncertainty from 10% to 20% results in a decrease in sensitivity of approximately 8% for all mixing parameters.

Optimized flux. In this section, we exclusively use the tau optimized flux configurations with an exposure of $3.5 + 3.5$ years for investigating the sensitivity and correlation among the standard physics parameters as obtained from the ν_τ appearance channel only.

From figure 4 we see that an increase in the tau detection efficiency or even in the S/B ratio impacts the parameters sensitivities less than in the case of the standard flux, the reason being that the flux is already optimized for tau as to produce a larger statistics in all cases. Analizing the correlation plots, we observe that the smallest allowed ranges found in the case of the standard flux can be further reduced up to 10% for θ_{23} and 15% for θ_{13} if the optimized flux is considered. Notice also that with such a flux, DUNE can reach a relative uncertainty of 4.5% in the measurement of the atmospheric mass difference if 10% systematics on the signal is assumed.
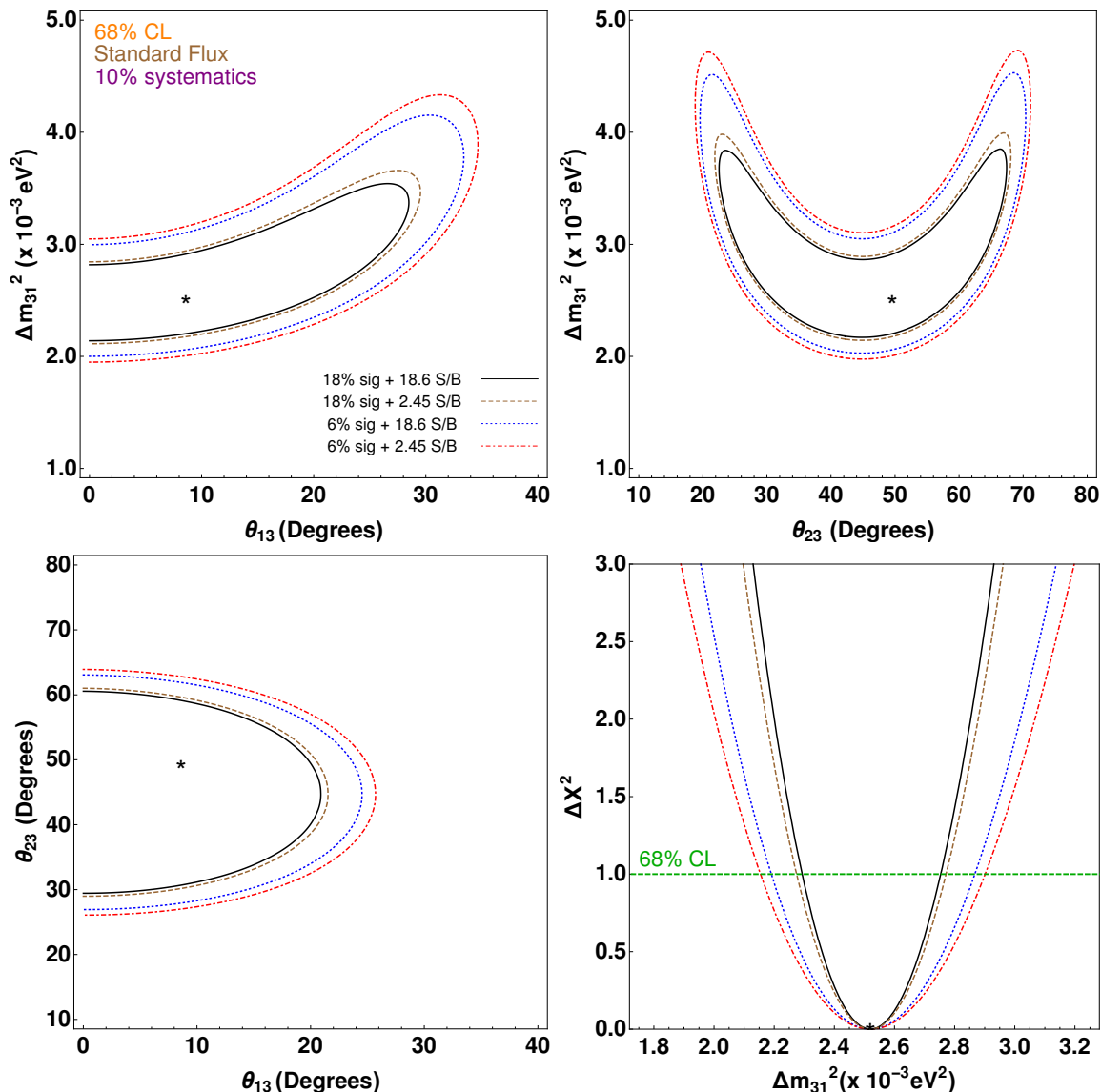
Figure 2. Expected contours at 68% CL in the oscillation parameter planes (as mentioned in each graph axis) for $S/B = 2.45$, with ν_τ detection efficiency of 6% (Red, DotDashed) and 18% (Brown, Dashed) and for $S/B = 18.6$ with ν_τ detection efficiency of 6% (Blue, Dotted) and 18% (Black, Solid). Standard flux has been assumed in the simulation, using only the ν_τ appearance channel in the Normal Hierarchy case with a 10% signal uncertainty. Marginalization over all undisplayed parameters has been performed. For the bottom right graph, $\Delta\chi^2 = \chi^2 - \chi^2_{\min}$ as a function of the true Δm^2_{31} is plotted. Stars represent the simulated true values.

Finally, in figure 5 we present the results obtained for a 20% signal uncertainty. As before, the improvement in the sensitivity is smaller than in the case of the standard flux. The parameter which is affected the most by the systematics is the atmospheric mass splitting whose relative uncertainty is roughly 10%.
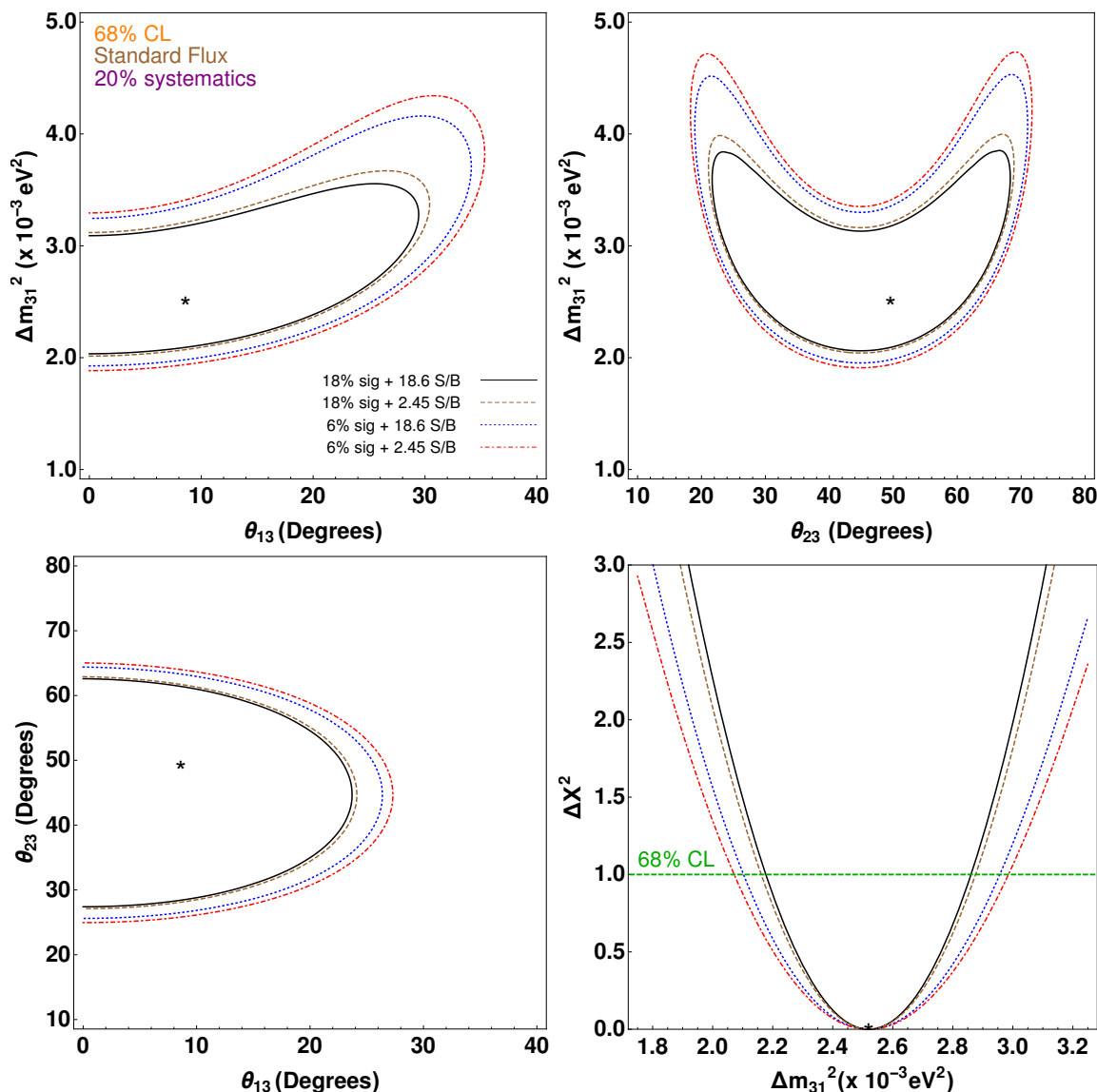
Figure 3. Same as figure 2 but with 20% signal uncertainty.

4 The case of Non-Standard Interaction

Several neutrino experiments have led to the opening for several new physics scenarios among which NSIs are quite popular. If the SM is regarded as a low-energy effective theory of some higher theory in the UV, then BSM would enter as higher-dimensional operators, suppressed by the new physics scale. In neutrino physics these are often written as four-fermion interactions, described by an effective four fermion Lagrangian [49]:

$$- \mathcal{L}_{\text{NSI}}^{\text{eff}} = \varepsilon_{\alpha\beta}^{fP} 2\sqrt{2} G_F (\bar{\nu}_\alpha \gamma_\rho L \nu_\beta)(\bar{f} \gamma^\rho P f) , \tag{4.1}$$

where G_F is the Fermi constant, $\varepsilon_{\alpha\beta}^{fP}$ is the parameter which describes the strength of the NSI, f is a first generation SM fermion (e, u or d), P denotes the chiral projector $\{L, R = (1 \pm \gamma^5)/2\}$, and α and β denote the neutrino flavors e, μ or τ.
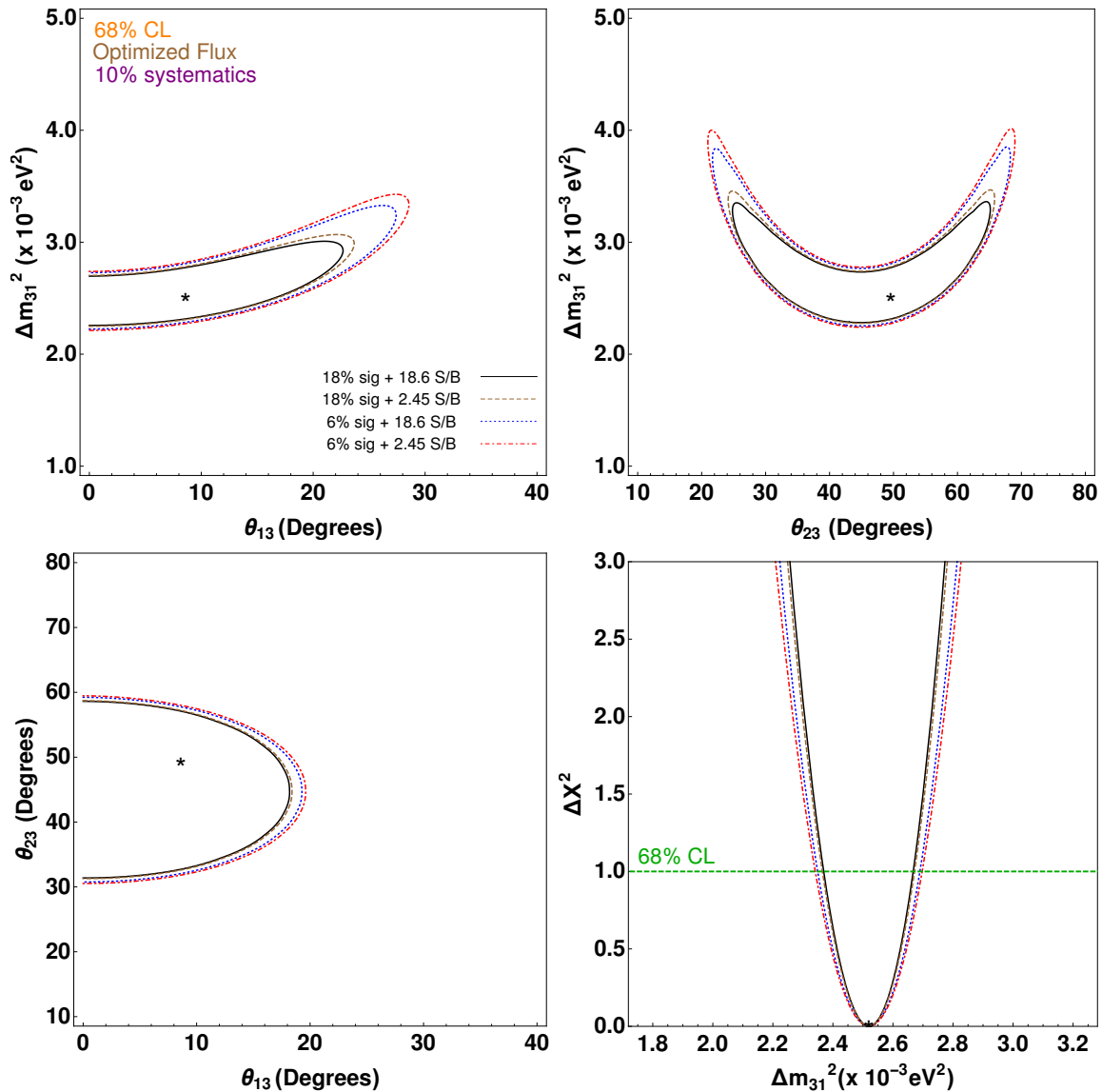
Figure 4. Expected contours at 68% CL in the oscillation parameter planes (as mentioned in each graph axis) for $S/B = 2.45$, with ν_τ detection efficiency of 6% (Red, DotDashed) and 18% (Brown, Dashed) and for $S/B = 18.6$ with ν_τ detection efficiency of 6% (Blue, Dotted) and 18% (Black, Solid). The tau optimized flux has been assumed in the simulation, using only the ν_τ appearance channel in the Normal Hierarchy case with a 10% signal uncertainty. Marginalization over all undisplayed parameters has been performed. For the bottom right graph, $\Delta\chi^2 = \chi^2 - \chi^2_{\min}$ as a function of the true Δm^2_{31} is plotted. Stars represent the simulated true values.

What is relevant for neutrino propagation in matter is the vector part V of interaction $\varepsilon^{fV}_{\alpha\beta} = \varepsilon^{fL}_{\alpha\beta} + \varepsilon^{fR}_{\alpha\beta}$ since the neutrino propagation in a medium is sensitive to the combination $\varepsilon_{\alpha\beta} = \varepsilon^{eV}_{\alpha\beta} + N_u/N_e \, \varepsilon^{uV}_{\alpha\beta} + N_d/N_e \, \varepsilon^{dV}_{\alpha\beta}$. Following what is usually done in the literature, we discuss the bounds from DUNE in terms of $\varepsilon_{\alpha\beta}$. Overall, this Lagrangian describes neutral current (NC) interactions; it basically modifies the matter Hamiltonian and consequently
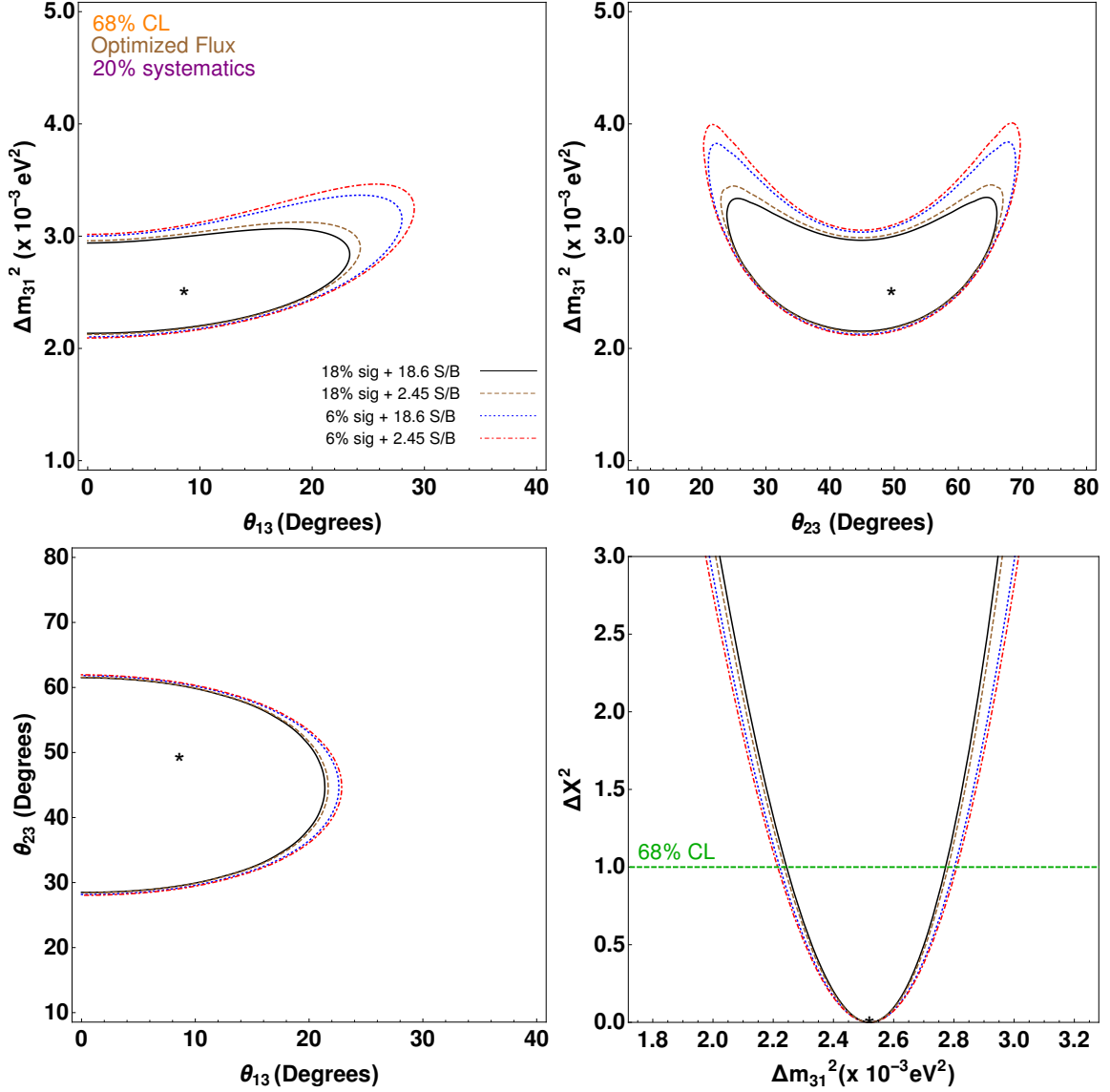
Figure 5. Same as figure 4 but with 20% signal uncertainty.

the transition probability of the neutrinos in matter. The strength of the new interaction is parameterized in terms of the complex $\varepsilon_{\alpha\beta} = |\epsilon_{\alpha\beta}|e^{i\phi_{\alpha\beta}}$ couplings. Thus the state evolution equations are given by:

$$i\frac{d}{dt}\begin{pmatrix} \nu_e \\ \nu_\mu \\ \nu_\tau \end{pmatrix} = \left[U_{PMNS} \begin{pmatrix} 0 & 0 & 0 \\ 0 & \Delta_{21} & 0 \\ 0 & 0 & \Delta_{31} \end{pmatrix} U_{PMNS}^\dagger + A \begin{pmatrix} 1+\epsilon_{ee} & \epsilon_{e\mu} & \epsilon_{e\tau} \\ \epsilon_{e\mu}^* & \epsilon_{\mu\mu} & \epsilon_{\mu\tau} \\ \epsilon_{e\tau}^* & \epsilon_{\mu\tau}^* & \epsilon_{\tau\tau} \end{pmatrix} \right] \begin{pmatrix} \nu_e \\ \nu_\mu \\ \nu_\tau \end{pmatrix} , \quad (4.2)$$

where $\Delta_{ij} = \Delta m_{ij}^2/2E$, U_{PMNS} is the neutrino mixing matrix, $A \equiv 2\sqrt{2}G_F n_e$ with n_e being the electron density in the Earth crust. All in all, beside the standard oscillation parameters, the parameter space is enriched by six more moduli $|\epsilon_{\alpha\beta}|$ and three more phases $\phi_{\alpha\beta}$.

NSI parameters	Limits
$\epsilon_{ee} - \epsilon_{\mu\mu}$	$(-0.2, 0.45)$
$|\epsilon_{e\mu}|$	< 0.1
$|\epsilon_{e\tau}|$	< 0.3
$\epsilon_{\tau\tau} - \epsilon_{\mu\mu}$	$(-0.02, 0.175)$
$|\epsilon_{\mu\tau}|$	< 0.03

Table 5. Current constraints on the NSI parameters at 90% CL obtained from a global fit to neutrino oscillation data [52]. No bounds on the phases $\phi_{\alpha\beta}$ are available so far.

Direct constraints on NSI can be derived from scattering processes [50] and from neutrino oscillation data [51]. Latest constrains on NSI parameters from global fits were quoted in [52], from which we extracted the limits reported in table 5, used in our numerical analysis. We want to outline that, in order to compute the oscillation probabilities in presence of NSI, we may subtract from the diagonal entries any one of the diagonal elements $\epsilon_{\alpha\alpha}$ as the oscillation phenomenon is insensitive to overall factors. Therefore one may consider, as done in table 5, the *shifted* parameters $\epsilon_{ee} - \epsilon_{\mu\mu}$ and $\epsilon_{\tau\tau} - \epsilon_{\mu\mu}$ instead of ϵ_{ee} and $\epsilon_{\tau\tau}$ respectively and set $\epsilon_{\mu\mu}$ to 0, which is also motivated by the strong external bounds as well [53].

4.1 The importance of $\nu_\mu \to \nu_\tau$ channel

General NSI considerations were already investigated in refs. [5, 6] and the effect of systematics were studied in [54] in the standard DUNE scenario consisting of the ν_e appearance and ν_μ disappearance channels. The $\nu_\mu \to \nu_e$ oscillation probability is affected by the $\epsilon_{e\mu}$ and $\epsilon_{e\tau}$ parameters, as well as by ϵ_{ee}. However, statistics in DUNE is dominated by the disappearance channel $\nu_\mu \to \nu_\mu$ which is mainly affected by the presence of $\epsilon_{\tau\tau}$ and $\epsilon_{\mu\tau}$. The dependence of probabilities on these parameters have been studied, among others, in [55–57].

For the appearance probability $\nu_\mu \to \nu_\tau$, the leading analytic behavior in terms of the small ϵ parameters is given by [56]:

$$P_{\mu\tau} = P_{\mu\tau}^{SM} + \left(\frac{1}{2}\epsilon_{\tau\tau}\cos^2(2\theta_{23}) + 2\cos(2\theta_{23})\text{Re}\{\epsilon_{\mu\tau}\} \right)(AL)\sin\left(\frac{\Delta m_{31}^2 L}{2E} \right) + \mathcal{O}(\epsilon^2), \quad (4.3)$$

where we neglected the small solar mass squared difference Δm_{21}^2; $P_{\mu\tau}^{SM}$ is the oscillation probability in absence of NSI already discussed in section 3. Additional terms, which depend on both the real and imaginary parts of $\epsilon_{\mu\tau}$, are at second order in the perturbative expansion, and are expected to provide only small sensitivity in the regions with $\phi_{\mu\tau} \sim \pm\pi/2$. Since the term containing $\epsilon_{\tau\tau}$ is very small for an almost maximal atmospheric angle, the probability $P_{\mu\tau}$ is sensitive to large values of $\epsilon_{\tau\tau}$ only, unlike for $\epsilon_{\mu\tau}$ to which we expect a maximal sensitivity.

4.2 Effect of systematics, experimental reach and ν_τ detection efficiency

In figures 6 and 7 we report the $\Delta\chi^2$ as a function of $|\epsilon_{\mu\tau}|$ for 10% (left panel) and 20% (right panel) systematic uncertainties for the ν_τ signal, for the standard and optimized
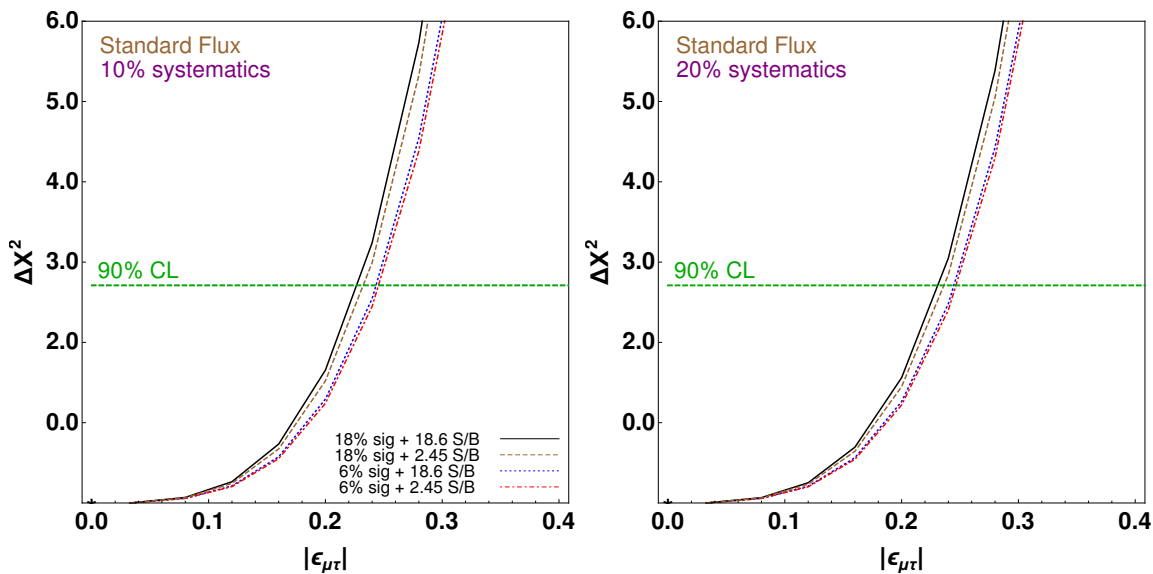
Figure 6. $\Delta\chi^2$ vs $|\epsilon_{\mu\tau}|$ for 10% (left panel) and 20% (right panel) ν_τ signal systematic uncertainty. The standard neutrino flux has been assumed in the simulations. Horizontal dashed line indicates the 90 % CL limit (1 degree of freedom). The meaning of the curves is the same as the previous plots.
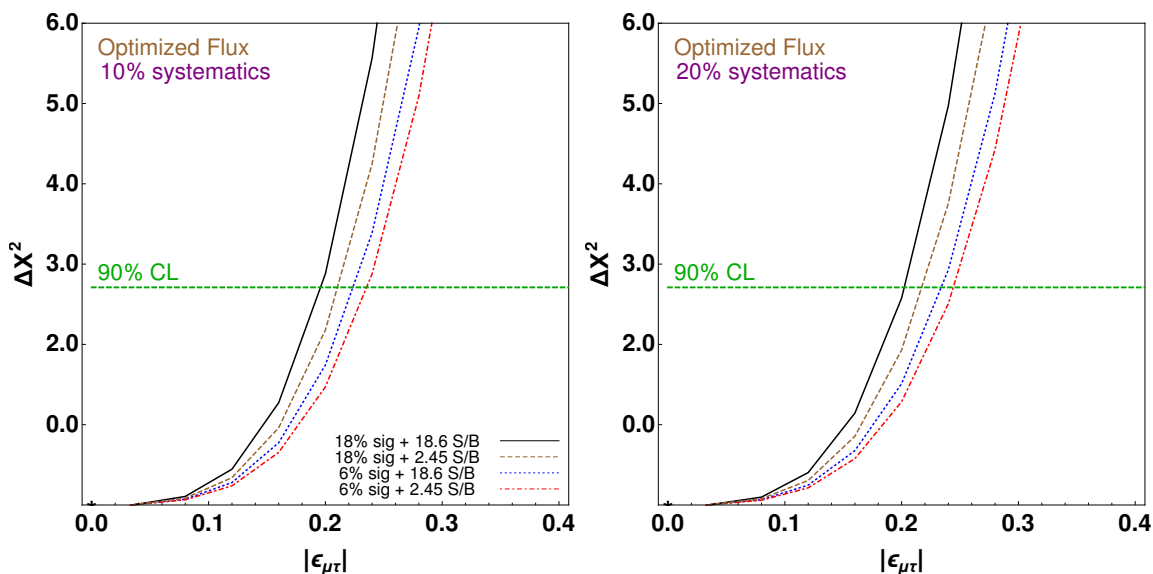

Figure 7. Same as figure 6 but for the optimized flux.

fluxes, respectively. Plots have been obtained marginalizing over all standard and non standard parameters according to the constraints reported in tables 2 and 5, except for the solar parameters θ_{12} and Δm_{21}^2 and the NSI parameter $\varepsilon_{\mu\tau}$, which have been fixed to their best fit values. All the NSI phases have been left free with no bounds.

	Standard Flux (10% sys)			
	S/B = 2.45		S/B = 18.6	
Efficiency of ν_τ detection	6%	18%	6%	18%
$|\epsilon_{\mu\tau}|$	[0,0.2452]	[0,0.2320]	[0,0.2431]	[0,0.2264]
	Optimized Flux (10% sys)			
	S/B = 2.45		S/B = 18.6	
Efficiency of ν_τ detection	6%	18%	6%	18%
$|\epsilon_{\mu\tau}|$	[0,0.2349]	[0,0.2101]	[0,0.2232]	[0,0.1955]

Table 6. Summary of 90% CL bounds on NSI parameter $|\epsilon_{\mu\tau}|$ that DUNE may set for 10% systematic uncertainty for the ν_τ appearance channel.

	Standard Flux (20% sys)			
	S/B = 2.45		S/B = 18.6	
Efficiency of ν_τ detection	6%	18%	6%	18%
$|\epsilon_{\mu\tau}|$	[0,0.2463]	[0,0.2359]	[0,0.2445]	[0,0.2306]
	Optimized Flux (20% sys)			
	S/B = 2.45		S/B = 18.6	
Efficiency of ν_τ detection	6%	18%	6%	18%
$|\epsilon_{\mu\tau}|$	[0,0.2440]	[0,0.2169]	[0,0.2335]	[0,0.2021]

Table 7. Same as table 6 but for a 20% systematic uncertainty for the ν_τ appearance channel.

The common feature of the above figures is that there is a significant improvement in the bound for $|\epsilon_{\mu\tau}|$ by increasing the efficiency from 6% upto 18%, and the S/B from 2.45 upto 18.6; one can envisage an overall improvement at 90% CL of approximately 10% in the parameter relative uncertainty in the case of the standard flux and 18% using the optimized flux.

Sensitivity limits at 90% CL reached with all the three appearance and disappearance channels in DUNE using the two fluxes are presented in the tables 6 and 7. The worst case scenario using the standard flux gives us a limit on the $|\epsilon_{\mu\tau}| \lesssim 0.25$ while the most stringent limit can be set using the optimized flux with the best efficiency (18%), the best

S/B (18.6) and 10% systematic uncertainty, $|\epsilon_{\mu\tau}| \lesssim 0.20$. This limit is approximately 35% smaller than the one that can be set by DUNE using only ν_e appearance and ν_μ disappearance channels with standard flux, $|\epsilon_{\mu\tau}| < 0.32$, as estimated in ref. [54]. We observe that a fit to the OPERA ν_τ events [32] did in ref. [48] predicted the bound $|\epsilon_{\mu\tau}| \lesssim$ 0.41 (marginalising over all parameters including NSI parameters) which is almost a factor of two larger than the worst limit DUNE can set.

We checked that the other NSI parameters do not benefit so much from the ν_τ appearance channel and the sensitivity reach remains roughly the same as in the standard DUNE scenario with ν_e appearance and ν_μ disappearance only.

5 The case of 3+1

The 3+1 sterile neutrino scenario is a possible solution to the short-baseline anomalies, which are about an excess of oscillations in short baseline experiments. For this reason, this new physics model is one of the most studied so far, and it is expected to be tested more in future experiments. The 3+1 sterile neutrino model is based on the addition of a fourth mass-eigenstate, m_4, to the other standard three. Furthermore, the new interaction eigenstate is assumed to be sterile, that is not involved in electro-weak interactions with matter.

Adding a new neutrino to the standard model introduces new parameters (three more mixing angles, θ_{14}, θ_{24} and θ_{34}, two more phases δ_1 and δ_3 and a new independent mass-squared splitting Δm_{41}^2) whose sensitivity will be studied in the following, with particular emphasis to the constraints attainable from the ν_τ appearance channel.

The U_{PMNS} matrix in this case is a unitary 4×4 matrix. The parameterization used here is as follows [58–60]:

$$U_{PMNS} = R(\theta_{34})\, R(\theta_{24})\, R(\theta_{23}, \delta_2)\, R(\theta_{14})\, R(\theta_{13}, \delta_3)\, R(\theta_{12}, \delta_1)\,, \tag{5.1}$$

where the phase δ_3 reduces to the standard δ_{CP} when the new mixing angles are set to zero. In our numerical simulations no external priors on the θ_{i4}'s have been considered.

5.1 The importance of $\nu_\mu \to \nu_\tau$ channel

The oscillation probabilities $\nu_\mu \to \nu_\tau$ in the case of the sterile neutrino model are more complicated than the standard ones. However in the vacuum it is possible to make some useful approximations (matter effects have been taken into account in the numerical simulations).

If the new mass-squared splitting satisfies $|\Delta m_{41}^2| \gg |\Delta m_{32}^2|$, it is possible to average all the trigonometric functions which include Δm_{41}^2. Using the additional approximation of vanishing Δm_{21}^2, the following $\nu_\mu \to \nu_\tau$ oscillation formula can be obtained:

$$P_{\mu\tau} = 2|U_{\tau4}|^2|U_{\mu4}|^2 + 4\Re[U_{\mu3}^* U_{\tau3}(U_{\mu3} U_{\tau3}^* + U_{\mu4} U_{\tau4}^*)]\sin^2\left(\frac{\Delta m_{32}^2 L}{4E}\right) +$$
$$- 2\Im(U_{\mu3}^* U_{\tau3} U_{\mu4} U_{\tau4}^*)\sin\left(\frac{\Delta m_{32}^2 L}{2E}\right)\,. \tag{5.2}$$

On the other hand, in the regime where $|\Delta m_{41}^2| \sim |\Delta m_{21}^2|$, an expansion to the first order in the small parameters $\alpha = \frac{\Delta m_{21}^2 L}{4E}$ and $\beta = \frac{\Delta m_{41}^2 L}{4E}$ produces the following result:

$$P_{\mu\tau} = 4\{|U_{\mu3}|^2|U_{\tau3}|^2 +$$
$$\Im[\alpha U_{\mu3}^* U_{\tau3} U_{\mu1} U_{\tau1}^* + (\beta - \alpha)U_{\mu4}^* U_{\tau4} U_{\mu3} U_{\tau3}^*]\}\sin^2\left(\frac{\Delta m_{32}^2 L}{4E}\right) +$$
$$- 2\Re[\alpha U_{\mu3}^* U_{\tau3} U_{\mu1} U_{\tau1}^* - (\beta - \alpha)U_{\mu4}^* U_{\tau4} U_{\mu3} U_{\tau3}^*]\sin\left(\frac{\Delta m_{32}^2 L}{2E}\right)\,. \tag{5.3}$$

Both eqs. (5.2) and (5.3) show that the $\nu_\mu \to \nu_\tau$ probability is driven by the combination $U_{\mu4}^* U_{\tau4}$ of new mixing angles that, as we have verified, does not appear in any of the other
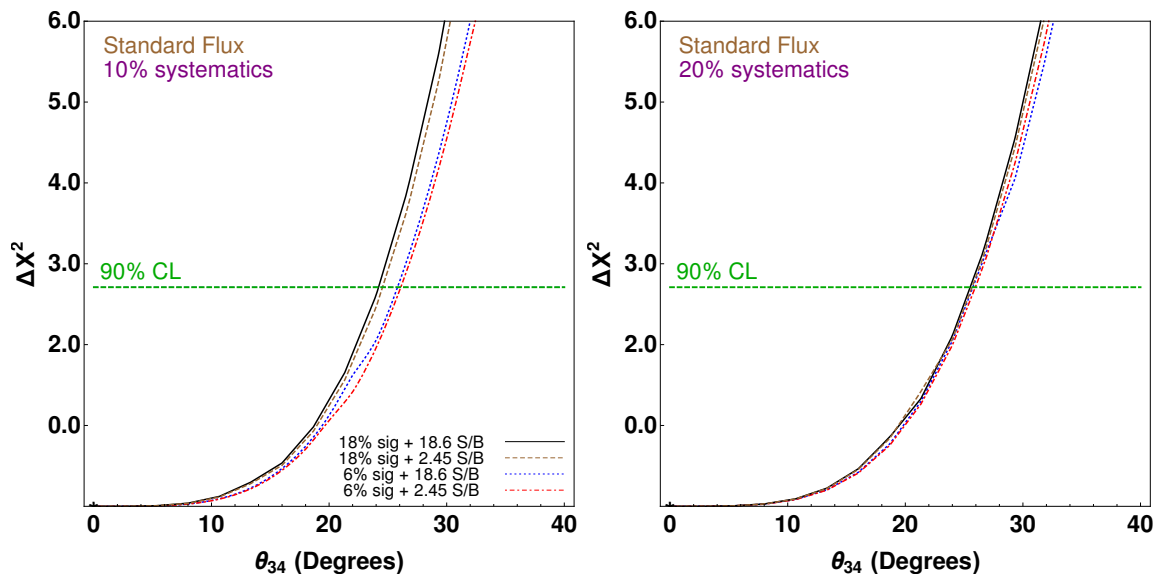
Figure 8. Expected sensitivity to θ_{34} obtained assuming the standard flux and $\Delta m_{41}^2 = 1\,\mathrm{eV}^2$. See text for more details.

oscillation probabilities at the leading order. In the parameterization used in this paper, such a combination can be written in terms of mixing angles as:

$$U_{\mu 4}^* U_{\tau 4} = \frac{1}{2} \cos^2 \theta_{14} \sin \theta_{34} \sin 2\theta_{24}. \tag{5.4}$$

This relation shows that the relevant changes in $P_{\mu\tau}$ with respect to the three neutrino scenario are mainly due to θ_{34} and θ_{24}. Since the combinations $U_{\mu 4}^* U_{e4}$ and $|U_{\mu 4}|^2$ that appear in the other oscillation probabilities contain θ_{24} as well [61–64], we expect θ_{34} to be the parameter whose sensitivity will be mostly affected by the addition of the ν_τ appearance channel.

5.2 Constraints on sterile neutrino parameters

In figures 8 (standard flux case) and 9 (optimized flux case) we show $\Delta\chi^2$ as a function of θ_{34} computed considering all available oscillation channels in DUNE, including the $\nu_\mu \to \nu_\tau$ transition. In the left panels we considered the case where a 10% of systematic uncertainty is assumed for the signal while the 20% case is illustrated in the right panel.

As in the previous sections, we present the four different cases corresponding to 6% of τ detection efficiency and $S/B = 2.45$ (Red, DotDashed), 18% efficiency and again

$S/B = 2.45$ (Brown, Dashed), 6% efficiency and $S/B = 18.6$ (Blue, Dotted) and 18% efficiency and $S/B = 18.6$ (Black, Solid). In the numerical simulations, the new physics parameters true values have been set to zero except for Δm_{41}^2 that has been fixed to $1\,\mathrm{eV}^2$. For the standard parameters we considered the central values and uncertainties reported in table 2. The mixing angles θ_{14} and θ_{24}, together with the two phases $\delta_{1,2}$ have been left free in the fit.
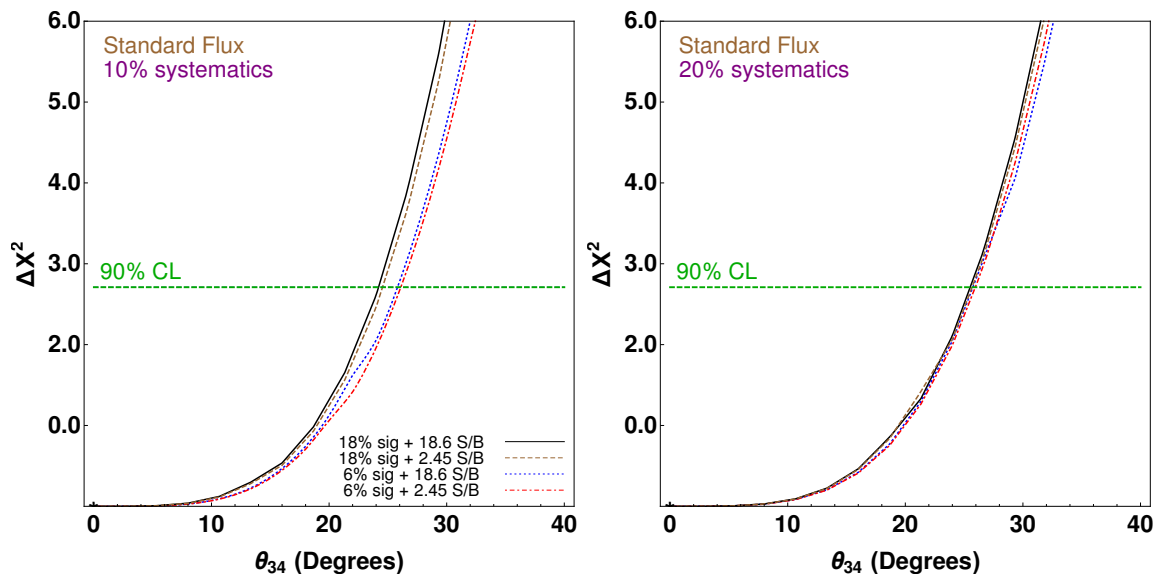
Figure 9. Same as figure 8 but for the optimized flux.

	Standard Flux (10% sys)			
	S/B = 2.45		S/B = 18.6	
Efficiency of ν_τ detection	6%	18%	6%	18%
θ_{34} ° $(\Delta m^2_{41} = 1\,\mathrm{eV}^2)$	[0, 26.07]	[0, 25.52]	[0, 24.78]	[0, 24.18]
	Optimized Flux (10% sys)			
	S/B = 2.45		S/B = 18.6	
Efficiency of ν_τ detection	6%	18%	6%	18%
θ_{34} ° $(\Delta m^2_{41} = 1\,\mathrm{eV}^2)$	[0, 23.93]	[0, 22.22]	[0, 23.47]	[0, 22.00]

Table 8. Summary of the bounds at 90% CL on θ_{34} (1 degree of freedom) that DUNE may set using 10% and systematic uncertainties.

From figures 8 and 9 we extracted the bounds at 90% CL on θ_{34} that we summarized in tables 8 and 9. As expected, the most stringent limit around 22° can be set using the optimized flux with the best efficiency (18%), the best S/B (18.6) and 10% systematic uncertainty, a result in line with the recent NC event analysis carried out in [65]. The importance of ν_τ appearance relies on the fact that such a limit would be roughly 20% smaller if only ν_e appearance and ν_μ disappearance channels with standard flux are considered, i.e 27.5°.

An important outcome of our analysis is that while the results with 10% systematic uncertainty and the optimized flux are always better than those obtained with the standard flux, for the 20% systematic this is not always the case; this is because the performances of the other two channels with optimized flux are worse, due to the increased number of ν_τ CC background events. Thus, even though the ν_τ appearance can help more in putting strong bounds for the optimized flux case, a larger systematic uncertainty brings to a regime where sensitivity limits are mainly set by the other two channels.

	Standard Flux (20% sys)			
	S/B = 2.45		S/B = 18.6	
Efficiency of ν_τ detection	6%	18%	6%	18%
θ_{34} ° $(\Delta m_{41}^2 = 1\,\mathrm{eV}^2)$	[0, 25.92]	[0, 25.64]	[0, 25.72]	[0, 25.49]
	Optimized Flux (20% sys)			
	S/B = 2.45		S/B = 18.6	
Efficiency of ν_τ detection	6%	18%	6%	18%
θ_{34} ° $(\Delta m_{41}^2 = 1\,\mathrm{eV}^2)$	[0, 26.81]	[0, 25.97]	[0, 26.64]	[0, 25.84]

Table 9. Same as table 8 but for a 20% systematic uncertainty for the ν_τ appearance channel.
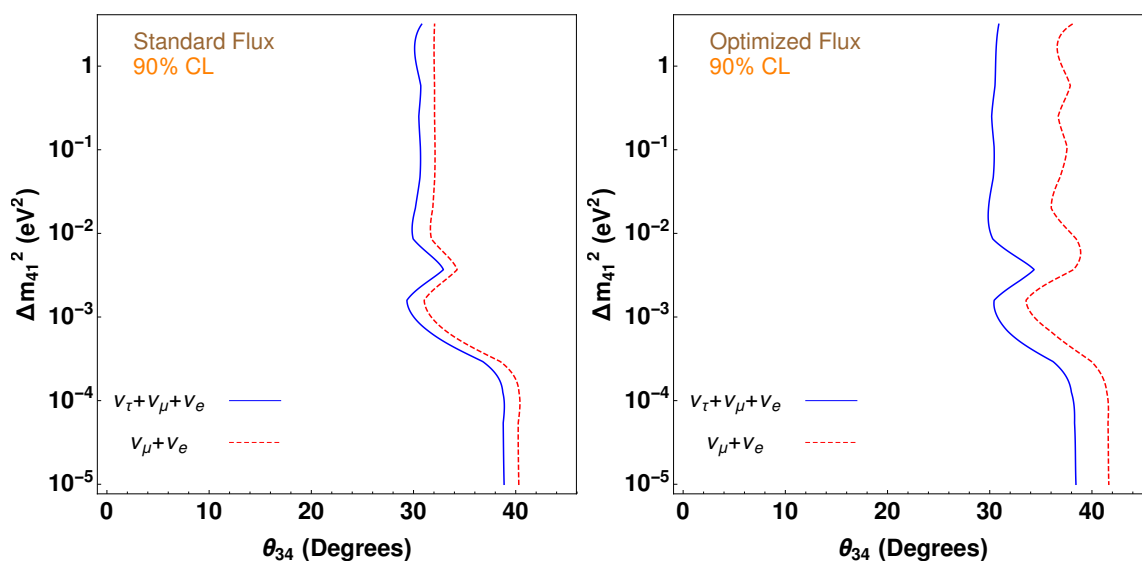

Figure 10. Expected contours at 90% CL in the $(\theta_{34}, \Delta m_{41}^2)$ plane, computed for the standard flux (left panel) and the optimized flux (right panel). The blue solid lines show the results obtained including the ν_τ appearance channel while the red dashed lines show the situation with no contribution of the τ channel. Detection efficiency is 6% with $S/B = 2.45$ and signal systematic uncertainty of 20%. All new physics parameters not shown have been left free in the simulation.

We complete our anaysis showing the correlation plots at 90% CL in several interesting planes. In all of them, the blue solid lines show the results obtained including the ν_τ appearance channel in the most conservative case, that is with a 6% τ detection efficiency, $S/B = 2.45$ and signal systematic uncertainty of 20%. The red dashed lines show the situation with no contribution of the τ channel but only ν_e appearance + ν_μ disappearance.

In figure 10 we focused on the $(\theta_{34}, \Delta m_{41}^2)$ plane; we clearly see that for both flux options the gain in sensitivity using the τ channel is not negligible, amounting to about 6% and 20% for the standard and optimized flux cases, respectively.

In figure 11 we show the correlation plots in the planes $(\theta_{34}, \theta_{14})$ (upper panels) and $(\theta_{34}, \theta_{24})$ (lower panels). The new mass difference Δm_{41}^2 is set to $10^{-5}\,\mathrm{eV}^2$ (left panels) and $1\,\mathrm{eV}^2$ (right panels) and the standard flux is assumed. First of all, we confirm that the
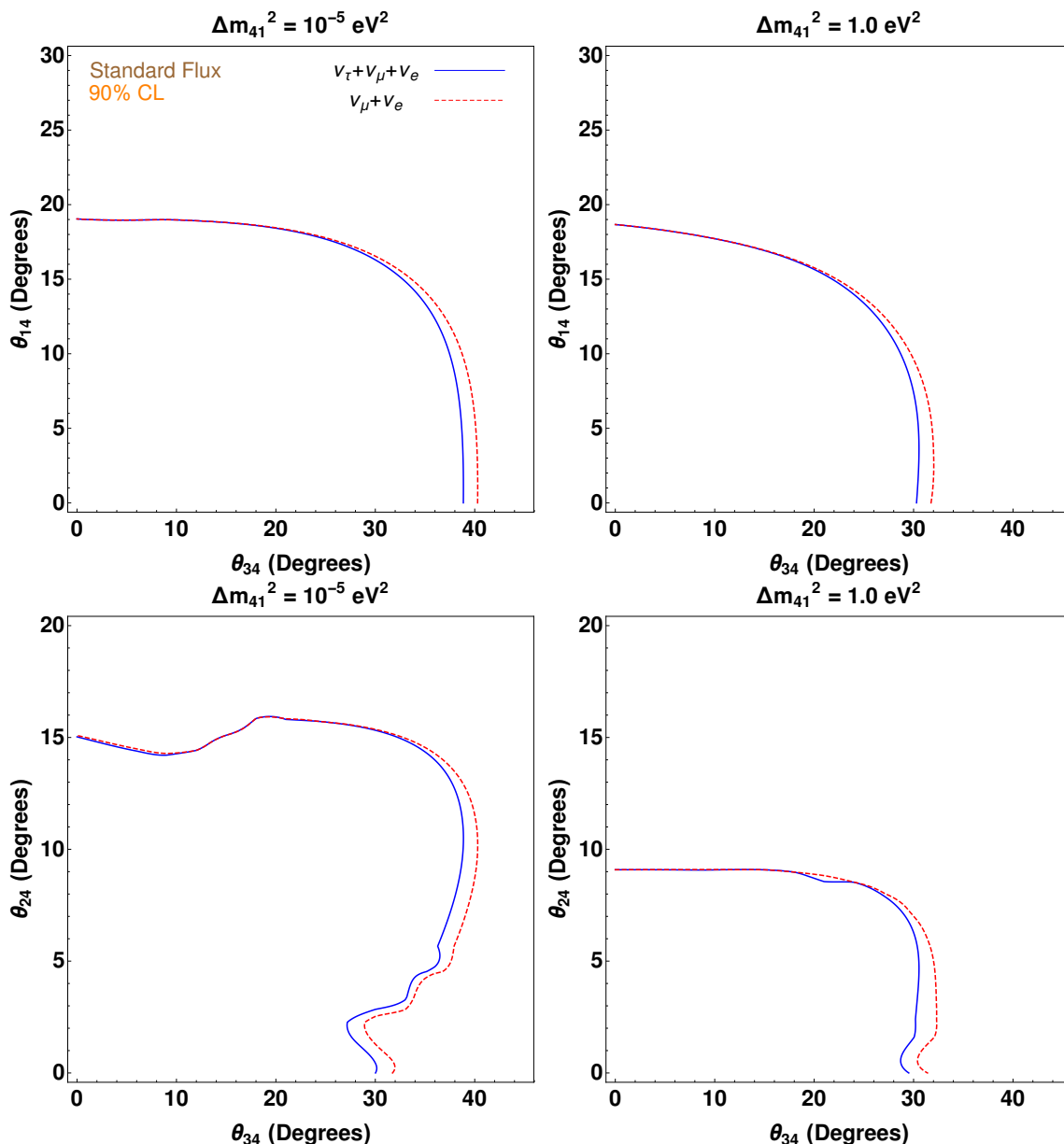
Figure 11. Same as figure 10 but in the planes $(\theta_{34}, \theta_{14})$ (upper panels) and $(\theta_{34}, \theta_{24})$ (lower panels). The new mass difference Δm_{41}^2 is set to two distinct values: $10^{-5}\,\text{eV}^2$ (left panels) and $1\,\text{eV}^2$ (right panels). Standard flux is assumed.

τ channel does not significantly improve the bounds on θ_{14} and θ_{24}, which are around $20°$ and between $10°$ and $20°$, respectively. Instead, the upper limit on θ_{34} can be improved by roughly 7% for both values of Δm_{41}^2 analyzed here. As for the absolute upper bound on θ_{34}, we observe that when the mass splitting is smaller, θ_{34} is confined to larger values because, as seen from the expression in eq. (5.3), in this mass regime the non standard matrix elements are always sub leading.
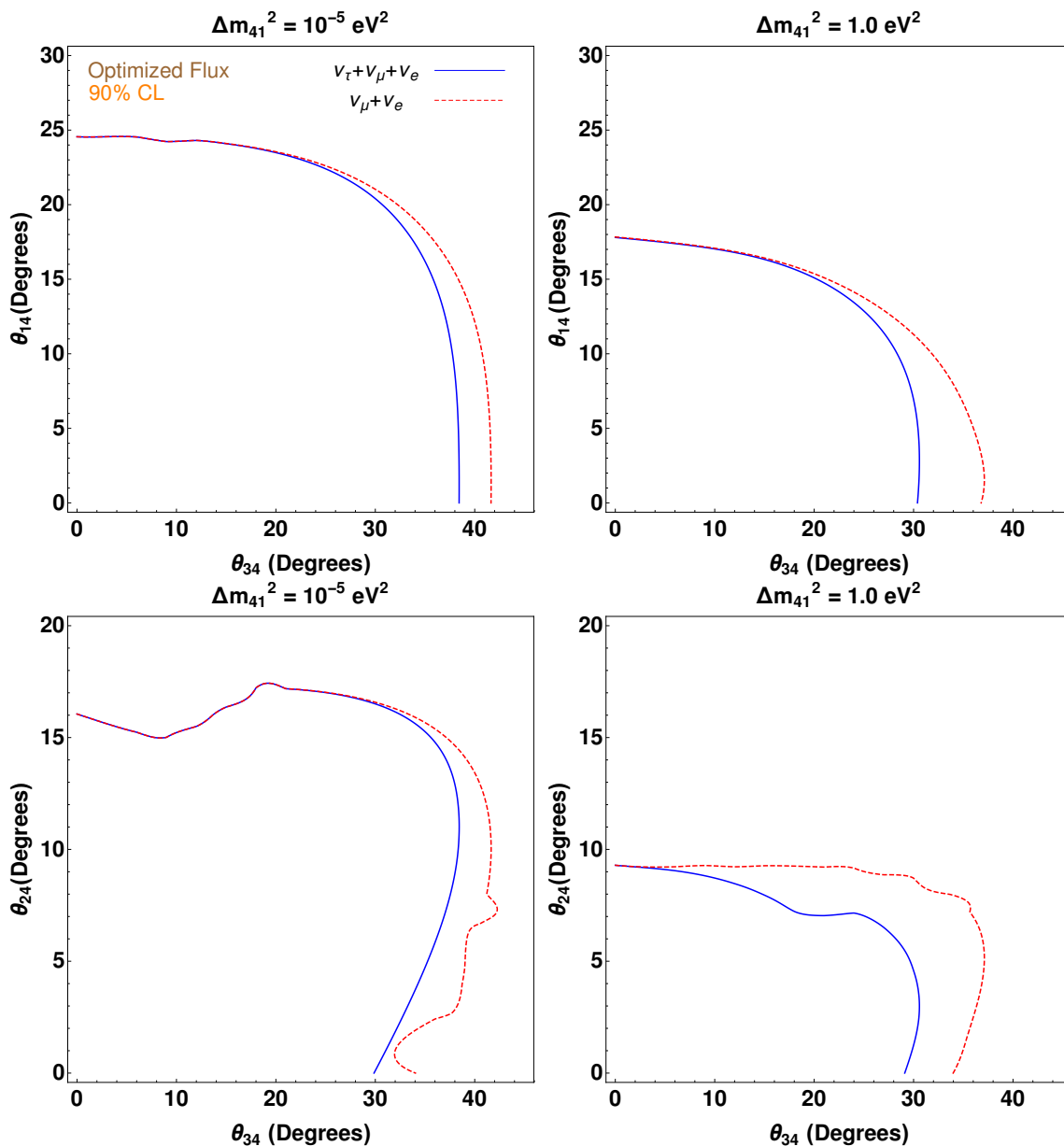
Figure 12. Same as figure 11 but for the optimized flux.

The situation where the optimized flux is taken into account is presented in figure 12; consistently with figure 10, the final sensitivity to θ_{34} when adding to the simulations all three transition channels is very similar to that obtained for the standard case. The real improvement carried by the optimized flux are on the (bad) limits set by ν_e appearance + ν_μ disappearance only, since they suffer by a large τ CC background. Finally, we comment on the fact that the sensitivities to the other sterile neutrino parameters are not affected at all by the addition of the ν_τ appearance channel.

6 Discussion and conclusions

The DUNE experiment is being proposed as a high precision next-generation neutrino experiment to be built in the USA. The baseline of DUNE is suitable for observing the neutrino mass hierarchy and measuring the CP phase δ_{CP} but only ν_e appearance and ν_μ disappearance have been considered in most of the analysis. We studied the impact of the inclusion of $\nu_\mu \to \nu_\tau$ and $\bar{\nu}_\mu \to \bar{\nu}_\tau$ channels in the DUNE experiment, considering the electronic τ decay mode. This oscillation channel is interesting because, on the one hand, it can confirm the three neutrino paradigm thanks to the redundancy produced by unitarity of the U_{PMNS} and, on the other hand, it can probe several scenarios of new physics thanks to the almost unique dependence of the transition probability on certain non-standard parameters.

Our simulations have taken into account the impact of various systematic uncertainties, ν_τ detection efficiencies, two different S/B ratios and two distinct neutrino fluxes on the sensitivities of the oscillation parameters. $(3.5 + 3.5)$ years of data taking for both flux options have been considered. Based on the simulations performed with the GLoBES software presented in sections 3, 4 and 5, we conclude the following:

- For the standard physics, the addition of ν_τ appearance channel does not improve the sensitivities of any of the neutrino oscillation parameter set by the other two channels already being considered in DUNE.

- The performances of the tau optimized flux in the ν_e appearance and ν_μ disappearance channels result generally in a worsening of the sensitivities, thus overshadowing the advantage one may get from the increase in the ν_τ statistics. This is mainly due to the increased background events in both the ν_e and ν_μ channels.

- In the new physics cases, the NSI parameter sensitivities are little affected by the addition of the new channel, except for the coupling $|\epsilon_{\mu\tau}|$ for which improved limits (about 15% better than the no-τ case) can be found.

- For the sterile neutrino 3+1 case, the only parameter that shows an increase in sensitivity is the mixing angle θ_{34} whose improvement is about 20% compared to the case where τ signal events are not considered.

We remark that it may be possible to improve the above-mentioned sensitivities if we add to this analysis the tau hadronic decay channel as well [34], which has a better ν_τ detection efficiency and consequently a bigger statistics.

Acknowledgments

References

[1] E. Roulet, *MSW effect with flavor changing neutrino interactions*, *Phys. Rev.* **D 44** (1991) R935 [INSPIRE].

[2] M.M. Guzzo, A. Masiero and S.T. Petcov, *On the MSW effect with massless neutrinos and no mixing in the vacuum*, *Phys. Lett.* **B 260** (1991) 154 [INSPIRE].

[3] Y. Farzan and M. Tortola, *Neutrino oscillations and Non-Standard Interactions*, *Front. Phys.* **6** (2018) 10 [arXiv:1710.09360] [INSPIRE].

[4] M. Masud, A. Chatterjee and P. Mehta, *Probing CP-violation signal at DUNE in presence of non-standard neutrino interactions*, *J. Phys.* **G 43** (2016) 095005 [arXiv:1510.08261] [INSPIRE].

[5] A. de Gouvêa and K.J. Kelly, *Non-standard Neutrino Interactions at DUNE*, *Nucl. Phys.* **B 908** (2016) 318 [arXiv:1511.05562] [INSPIRE].

[6] P. Coloma, *Non-Standard Interactions in propagation at the Deep Underground Neutrino Experiment*, *JHEP* **03** (2016) 016 [arXiv:1511.06357] [INSPIRE].

[7] K. Huitu, T.J. Kärkkäinen, J. Maalampi and S. Vihonen, *Constraining the nonstandard interaction parameters in long baseline neutrino experiments*, *Phys. Rev.* **D 93** (2016) 053016 [arXiv:1601.07730] [INSPIRE].

[8] M. Masud and P. Mehta, *Nonstandard interactions spoiling the CP-violation sensitivity at DUNE and other long baseline experiments*, *Phys. Rev.* **D 94** (2016) 013014 [arXiv:1603.01380] [INSPIRE].

[9] M. Blennow, S. Choubey, T. Ohlsson, D. Pramanik and S.K. Raut, *A combined study of source, detector and matter non-standard neutrino interactions at DUNE*, *JHEP* **08** (2016) 090 [arXiv:1606.08851] [INSPIRE].

[10] S. Fukasawa, M. Ghosh and O. Yasuda, *Sensitivity of the T2HKK experiment to nonstandard interactions*, *Phys. Rev.* **D 95** (2017) 055005 [arXiv:1611.06141] [INSPIRE].

[11] J. Liao, D. Marfatia and K. Whisnant, *Nonstandard neutrino interactions at DUNE, T2HK and T2HKK*, *JHEP* **01** (2017) 071 [arXiv:1612.01443] [INSPIRE].

[12] S. Verma and S. Bhardwaj, *Non-standard interactions and parameter degeneracies in DUNE and T2HKK*, arXiv:1808.04263 [INSPIRE].

[13] LSND collaboration, *Candidate events in a search for $\bar{\nu}_\mu \to \bar{\nu}_e$ oscillations*, *Phys. Rev. Lett.* **75** (1995) 2650 [nucl-ex/9504002] [INSPIRE].

[14] LSND collaboration, *Evidence for neutrino oscillations from the observation of anti-neutrino(electron) appearance in a anti-neutrino(muon) beam*, *Phys. Rev.* **D 64** (2001) 112007 [hep-ex/0104049] [INSPIRE].

[15] MiniBooNE collaboration, *Significant Excess of ElectronLike Events in the MiniBooNE Short-Baseline Neutrino Experiment*, *Phys. Rev. Lett.* **121** (2018) 221801 [arXiv:1805.12028] [INSPIRE].

[16] S.K. Agarwalla, S.S. Chatterjee, A. Dasgupta and A. Palazzo, *Discovery Potential of T2K and NOvA in the Presence of a Light Sterile Neutrino*, *JHEP* **02** (2016) 111 [arXiv:1601.05995] [INSPIRE].

[17] S.K. Agarwalla, S.S. Chatterjee and A. Palazzo, *Physics Reach of DUNE with a Light Sterile Neutrino*, *JHEP* **09** (2016) 016 [arXiv:1603.03759] [INSPIRE].

[18] D. Dutta, R. Gandhi, B. Kayser, M. Masud and S. Prakash, *Capabilities of long-baseline experiments in the presence of a sterile neutrino*, *JHEP* **11** (2016) 122 [arXiv:1607.02152] [INSPIRE].

[19] NOvA collaboration, *Search for active-sterile neutrino mixing using neutral-current interactions in NOvA*, *Phys. Rev.* **D 96** (2017) 072006 [arXiv:1706.04592] [INSPIRE].

[20] MINOS+ collaboration, *Search for sterile neutrinos in MINOS and MINOS+ using a two-detector fit*, *Phys. Rev. Lett.* **122** (2019) 091803 [arXiv:1710.06488] [INSPIRE].

[21] S. Choubey, D. Dutta and D. Pramanik, *Measuring the Sterile Neutrino CP Phase at DUNE and T2HK*, *Eur. Phys. J.* **C 78** (2018) 339 [arXiv:1711.07464] [INSPIRE].

[22] S.K. Agarwalla, S.S. Chatterjee and A. Palazzo, *Signatures of a Light Sterile Neutrino in T2HK*, *JHEP* **04** (2018) 091 [arXiv:1801.04855] [INSPIRE].

[23] S. Gupta, Z.M. Matthews, P. Sharma and A.G. Williams, *The Effect of a Light Sterile Neutrino at NOνA and DUNE*, *Phys. Rev.* **D 98** (2018) 035042 [arXiv:1804.03361] [INSPIRE].

[24] T. Thakore, M.M. Devi, S. Kumar Agarwalla and A. Dighe, *Active-sterile neutrino oscillations at INO-ICAL over a wide mass-squared range*, *JHEP* **08** (2018) 022 [arXiv:1804.09613] [INSPIRE].

[25] T2K collaboration, *Search for light sterile neutrinos with the T2K far detector Super-Kamiokande at a baseline of 295 km*, *Phys. Rev.* **D 99** (2019) 071103 [arXiv:1902.06529] [INSPIRE].

[26] DUNE collaboration, *Long-Baseline Neutrino Facility (LBNF) and Deep Underground Neutrino Experiment (DUNE) Conceptual Design Report Volume 1: The LBNF and DUNE Projects*, arXiv:1601.05471 [INSPIRE].

[27] DUNE collaboration, *Long-Baseline Neutrino Facility (LBNF) and Deep Underground Neutrino Experiment (DUNE) Conceptual Design Report Volume 2: The Physics Program for DUNE at LBNF*, arXiv:1512.06148 [INSPIRE].

[28] DUNE collaboration, *Long-Baseline Neutrino Facility (LBNF) and Deep Underground Neutrino Experiment (DUNE) Conceptual Design Report Volume 3: Long-Baseline Neutrino Facility for DUNE June 24, 2015*, arXiv:1601.05823 [INSPIRE].

[29] DUNE collaboration, *Experiment Simulation Configurations Used in DUNE CDR*, arXiv:1606.09550 [INSPIRE].

[30] OPERA collaboration, *Evidence for $\nu_\mu \to \nu_\tau$ appearance in the CNGS neutrino beam with the OPERA experiment*, *Phys. Rev.* **D 89** (2014) 051102 [arXiv:1401.2079] [INSPIRE].

[31] G. Galati et al., *More results from the OPERA experiment*, *Nuovo Cim.* **C 40** (2017) 160 [INSPIRE].

[32] OPERA collaboration, *Final Results of the OPERA Experiment on ν_τ Appearance in the CNGS Neutrino Beam*, *Phys. Rev. Lett.* **120** (2018) 211801 [*Erratum ibid.* **121** (2018) 139901] [arXiv:1804.04912] [INSPIRE].

[33] A. Rashed and A. Datta, *Determination of mass hierarchy with $\nu_\mu \to \nu_\tau$ appearance and the effect of nonstandard interactions*, *Int. J. Mod. Phys.* **A 32** (2017) 1750060 [arXiv:1603.09031] [INSPIRE].

[34] A. De Gouvêa, K.J. Kelly, G.V. Stenico and P. Pasquini, *Physics with Beam Tau-Neutrino Appearance at DUNE*, *Phys. Rev.* **D 100** (2019) 016004 [arXiv:1904.07265] [INSPIRE].

[35] P. Huber, M. Lindner and W. Winter, *Simulation of long-baseline neutrino oscillation experiments with GLoBES (General Long Baseline Experiment Simulator)*, *Comput. Phys. Commun.* **167** (2005) 195 [hep-ph/0407333] [INSPIRE].

[36] P. Huber, J. Kopp, M. Lindner, M. Rolinec and W. Winter, *New features in the simulation of neutrino oscillation experiments with GLoBES 3.0: General Long Baseline Experiment Simulator*, *Comput. Phys. Commun.* **177** (2007) 432 [hep-ph/0701187] [INSPIRE].

[37] http://home.fnal.gov/~ljf26/DUNEFluxes/.

[38] M. Bishai and M. Dolce, *Optimization of the LBNF/DUNE beamline for tau neutrinos*, in Document Database (DocDB) for DUNE and LBNF [http://docs.dunescience.org/cgi-bin/RetrieveFile?docid=2013&filename=DOLCE_M_report.pdf&version=1].

[39] PARTICLE DATA GROUP collaboration, *Review of Particle Physics*, *Phys. Rev.* **D 98** (2018) 030001 [INSPIRE].

[40] P. Aprili et al., *ICARUS: a second generation proton decay experiment and neutrino observatory at the Gran Sasso Laboratory*, CERN-SPSC-2002-027 (2002).

[41] V.D. Barger, A.M. Gago, D. Marfatia, W.J.C. Teves, B.P. Wood and R. Zukanovich Funchal, *Neutrino oscillation parameters from MINOS, ICARUS and OPERA combined*, *Phys. Rev.* **D 65** (2002) 053016 [hep-ph/0110393] [INSPIRE].

[42] E.K. Akhmedov, R. Johansson, M. Lindner, T. Ohlsson and T. Schwetz, *Series expansions for three flavor neutrino oscillation probabilities in matter*, *JHEP* **04** (2004) 078 [hep-ph/0402175] [INSPIRE].

[43] I. Esteban, M.C. Gonzalez-Garcia, A. Hernandez-Cabezudo, M. Maltoni and T. Schwetz, *Global analysis of three-flavour neutrino oscillations: synergies and tensions in the determination of θ_{23}, δ_{CP} and the mass ordering*, *JHEP* **01** (2019) 106 [arXiv:1811.05487] [INSPIRE].

[44] P. Huber, M. Lindner and W. Winter, *Superbeams versus neutrino factories*, *Nucl. Phys.* **B 645** (2002) 3 [hep-ph/0204352] [INSPIRE].

[45] G.L. Fogli, E. Lisi, A. Marrone, D. Montanino and A. Palazzo, *Getting the most from the statistical analysis of solar neutrino oscillations*, *Phys. Rev.* **D 66** (2002) 053010 [hep-ph/0206162] [INSPIRE].

[46] A.M. Ankowski and C. Mariani, *Systematic uncertainties in long-baseline neutrino-oscillation experiments*, *J. Phys.* **G 44** (2017) 054001 [arXiv:1609.00258] [INSPIRE].

[47] V. De Romeri, E. Fernandez-Martinez and M. Sorel, *Neutrino oscillations at DUNE with improved energy reconstruction*, *JHEP* **09** (2016) 030 [arXiv:1607.00293] [INSPIRE].

[48] D. Meloni, *Exploring new physics from ν_τ events in OPERA*, *Phys. Lett.* **B 792** (2019) 199 [arXiv:1903.08933] [INSPIRE].

[49] S. Davidson, C. Pena-Garay, N. Rius and A. Santamaria, *Present and future bounds on nonstandard neutrino interactions*, *JHEP* **03** (2003) 011 [hep-ph/0302093] [INSPIRE].

[50] C. Biggio, M. Blennow and E. Fernandez-Martinez, *General bounds on non-standard neutrino interactions*, *JHEP* **08** (2009) 090 [arXiv:0907.0097] [INSPIRE].

[51] M.C. Gonzalez-Garcia and M. Maltoni, *Determination of matter potential from global analysis of neutrino oscillation data*, *JHEP* **09** (2013) 152 [arXiv:1307.3092] [INSPIRE].

[52] I. Esteban, M.C. Gonzalez-Garcia and M. Maltoni, *On the Determination of Leptonic CP-violation and Neutrino Mass Ordering in Presence of Non-Standard Interactions: Present Status*, *JHEP* **06** (2019) 055 [arXiv:1905.05203] [INSPIRE].

[53] T. Ohlsson, *Status of non-standard neutrino interactions*, *Rept. Prog. Phys.* **76** (2013) 044201 [arXiv:1209.2710] [INSPIRE].

[54] D. Meloni, *On the systematic uncertainties in DUNE and their role in New Physics studies*, *JHEP* **08** (2018) 028 [arXiv:1805.01747] [INSPIRE].

[55] J. Kopp, M. Lindner, T. Ota and J. Sato, *Non-standard neutrino interactions in reactor and superbeam experiments*, *Phys. Rev.* **D 77** (2008) 013007 [arXiv:0708.0152] [INSPIRE].

[56] T. Kikuchi, H. Minakata and S. Uchinami, *Perturbation Theory of Neutrino Oscillation with Nonstandard Neutrino Interactions*, *JHEP* **03** (2009) 114 [arXiv:0809.3312] [INSPIRE].

[57] M. Blennow, D. Meloni, T. Ohlsson, F. Terranova and M. Westerberg, *Non-standard interactions using the OPERA experiment*, *Eur. Phys. J.* **C 56** (2008) 529 [arXiv:0804.2744] [INSPIRE].

[58] M. Maltoni and T. Schwetz, *Sterile neutrino oscillations after first MiniBooNE results*, *Phys. Rev.* **D 76** (2007) 093005 [arXiv:0705.0107] [INSPIRE].

[59] A. Donini, M. Maltoni, D. Meloni, P. Migliozzi and F. Terranova, *3+1 sterile neutrinos at the CNGS*, *JHEP* **12** (2007) 013 [arXiv:0704.0388] [INSPIRE].

[60] D. Meloni, J. Tang and W. Winter, *Sterile neutrinos beyond LSND at the Neutrino Factory*, *Phys. Rev.* **D 82** (2010) 093008 [arXiv:1007.2419] [INSPIRE].

[61] A. Donini, K.-i. Fuki, J. Lopez-Pavon, D. Meloni and O. Yasuda, *The discovery channel at the Neutrino Factory: $\nu_\mu \to \nu_\tau$ pointing to sterile neutrinos*, *JHEP* **08** (2009) 041 [arXiv:0812.3703] [INSPIRE].

[62] N. Klop and A. Palazzo, *Imprints of CP-violation induced by sterile neutrinos in T2K data*, *Phys. Rev.* **D 91** (2015) 073017 [arXiv:1412.7524] [INSPIRE].

[63] J.M. Berryman, A. de Gouvêa, K.J. Kelly and A. Kobach, *Sterile neutrino at the Deep Underground Neutrino Experiment*, *Phys. Rev.* **D 92** (2015) 073012 [arXiv:1507.03986] [INSPIRE].

[64] R. Gandhi, B. Kayser, M. Masud and S. Prakash, *The impact of sterile neutrinos on CP measurements at long baselines*, *JHEP* **11** (2015) 039 [arXiv:1508.06275] [INSPIRE].

[65] P. Coloma, D.V. Forero and S.J. Parke, *DUNE Sensitivities to the Mixing between Sterile and Tau Neutrinos*, *JHEP* **07** (2018) 079 [arXiv:1707.05348] [INSPIRE].